

Lead Optimization of 1,4-Azaindoles as Antimycobacterial Agents

Pravin S. Shirude,^{*,†,∞} Radha K. Shandil,[‡] M. R. Manjunatha,[†] Claire Sadler,[§] Manoranjan Panda,[†] Vijender Panduga,[‡] Jitendar Reddy,[‡] Ramanatha Saralaya,[‡] Robert Nanduri,[‡] Anisha Ambady,^{||} Sudha Ravishankar,^{||} Vasan K. Sambandamurthy,^{||} Vaishali Humnabadkar,^{||} Lalit K. Jena,[†] Rudrapatna S. Suresh,[†] Abhishek Srivastava,[‡] K. R. Prabhakar,[‡] James Whiteaker,[⊥] Robert E. McLaughlin,[⊥] Sreevalli Sharma,^{||} Christopher B. Cooper,[#] Khisi Mdluli,[#] Scott Butler,[⊥] Pravin S. Iyer,[†] Shridhar Narayanan,^{||} and Monalisa Chatterji^{*,||}

[†]Department of Medicinal Chemistry, iMED Infection, AstraZeneca, Bellary Road, Hebbal, Bangalore 560024, India

[‡]DMPK and Animal Sciences, iMED Infection, AstraZeneca, Hebbal, Bangalore 560024, India

[§]Safety Assessment, iMED, AstraZeneca, Alderly Park, Mereside SK10 4TG, United Kingdom

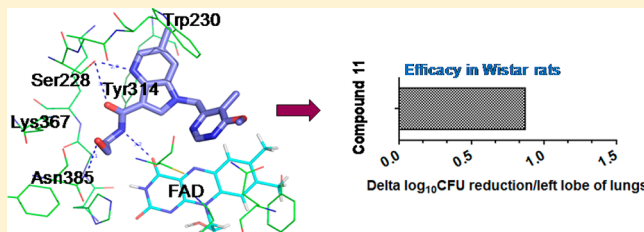
^{||}Department of Biosciences, iMED Infection, AstraZeneca, Hebbal, Bangalore 560024, India

[⊥]Infection iMED, AstraZeneca, GHP, Waltham, Massachusetts 02451, United States

[#]Global Alliance for TB Drug Development, New York, New York 10005, United States

Supporting Information

ABSTRACT: In a previous report, we described the discovery of 1,4-azaindoles, a chemical series with excellent in vitro and in vivo antimycobacterial potency through noncovalent inhibition of decaprenylphosphoryl- β -D-ribose-2'-epimerase (DprE1). Nevertheless, high mouse metabolic turnover and phosphodiesterase 6 (PDE6) off-target activity limited its advancement. Herein, we report lead optimization of this series, culminating in potent, metabolically stable compounds that have a robust pharmacokinetic profile without any PDE6 liability. Furthermore, we demonstrate efficacy for 1,4-azaindoles in a rat chronic TB infection model. We believe that compounds from the 1,4-azaindole series are suitable for in vivo combination and safety studies.



INTRODUCTION

Tuberculosis (TB) remains a global health emergency, as the WHO estimated 8.6 million TB cases and 1.3 million fatalities in 2012.¹ The current chemotherapy for the treatment of TB is more than 40 years old and has significant compliance challenges because of associated toxicities and the long duration of therapy.² The TB threat has acquired a new dimension with the appearance of multidrug-resistant TB (MDR-TB) and extensively drug-resistant TB (XDR-TB).² The treatment for drug-resistant TB is prolonged and challenging, with limited treatment options. Therefore, there is a dire need for new agents that work via novel mechanisms and that are effective in curing drug-resistant TB.

In an earlier report, we described the discovery of a novel and promising class of compounds, 1,4-azaindoles, that shows activity against *Mycobacterium tuberculosis* (Mtb) in vitro, ex vivo, and in mouse infection models of TB. Decaprenylphosphoryl- β -D-ribose-2'-epimerase (DprE1) of Mtb was identified as the target for azaindoles.³ DprE1 catalyzes the conversion of decaprenylphosphoryl- β -D-ribose (DPR) to decaprenylphosphoryl- β -D-arabinofuranose (DPA).⁴ DPA is an essential precursor of mycobacterial cell wall arabinan.⁴ Benzothiazinones, **1** (BTZ043)⁵ (Figure 1), and related compounds are

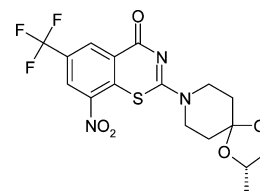


Figure 1. Structure of BTZ043 (**1**).⁵

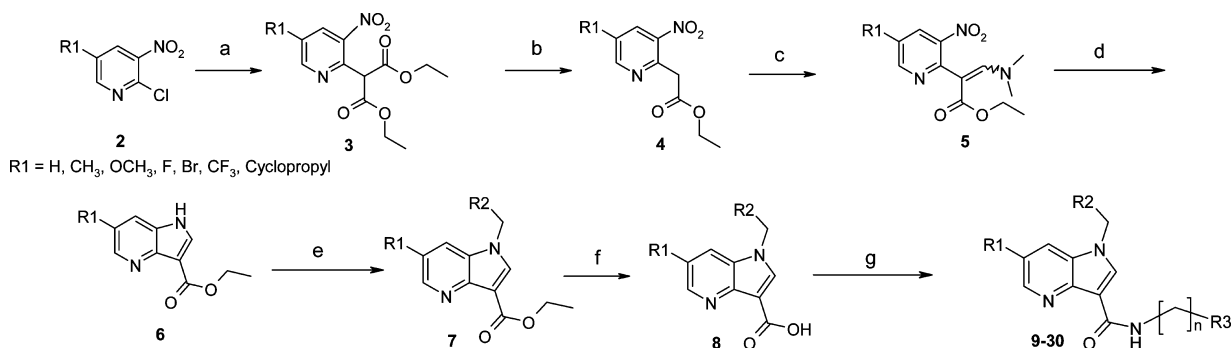
known covalent inhibitors of the DprE1 enzyme.⁵ Unlike benzothiazinones, azaindoles are noncovalent inhibitors and do not show cross-resistance to 1-resistant Mtb.³ In our previous report,³ we described developing a robust understanding of the cellular potency-based structure–activity relationship (SAR) for this series. The potent antimycobacterial activity, drug-like properties, lack of pre-existing resistance, and minimal in vitro safety liabilities encouraged us to develop 1,4-azaindoles toward a drug candidate shortlist.

This series was one of the first examples of a potent, noncovalent class of DprE1 inhibitors that demonstrated

Received: April 12, 2014

Table 1. Structure–Activity Relationship of 1,4-Azaindoles with Respect to PDE6 Activity

No	Structure	Mtb MIC (μM)	DprE1 IC ₅₀ (μM)	PDE6 IC ₅₀ (μM)	No	Structure	Mtb MIC (μM)	DprE1 IC ₅₀ (μM)	PDE6 IC ₅₀ (μM)
9		0.78	0.010	9	13		6.25	0.020	>100
10		0.39	0.005	3	14		<0.39	0.004	>100
11		<0.39	0.003	1	15		1.56	0.007	>100
12		1.56	0.010	6	16		1.56	0.019	>100

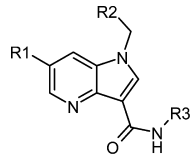
Scheme 1. Synthesis of 1,4-Azaindole Analogues^a

^aReagents and conditions: (a) diethyl malonate, NaH, THF, 80 °C, 50–80%; (b) LiCl, DMSO/H₂O, 80 °C, 70–80%; (c) DMF dimethylacetal, DMF, 80 °C, 60–70%; (d) Fe, acetic acid, 60 °C, 25–30%; (e) aryl halide, K₂CO₃, 60–70%; (f) LiOH, CH₃OH/H₂O, 60 °C, 70–80%; (g) amine, T3P, Et₃N or HATU, NMP, Et₃N, 70–80%.

efficacy in a rodent model of tuberculosis, making it promising for further development. However, there were two significant challenges associated with the series that still needed to be optimized. The *in vitro* secondary pharmacology profiling (a panel of 65 high- and medium-severity targets) of various compounds in the series identified PDE6 inhibition as a potential liability. PDE6 is expressed in rod and cone cells in the human eye. PDE6 inhibition is expected to have effects on visual acuity, which can have serious implications for a chronic therapy regimen such as that of TB.

Another significant challenge associated with the 1,4-azaindole series is low exposure in mice coupled with a poor pharmacokinetic (PK) profile. This suboptimal PK behavior could be correlated to rapid metabolism in the presence of mouse liver microsomes. This posed a major challenge in assessing efficacy in the mouse models of TB infection. Ultimately, we co-dosed our compounds with 1-amino-

benzotriazole (ABT), a pan-inhibitor of CYP isoforms, in order to achieve efficacious exposures by blocking mouse-specific clearance. Interestingly, the intrinsic clearance in other species, including humans, was predicted to be more favorable, as assessed by a comparatively low compound turnover in the presence of microsomes and hepatocytes from rat, dog, and human, demonstrating that this was a mouse-specific challenge.³ To mitigate high mouse clearance, during our lead optimization program we attempted to identify analogues with improved oral exposure in mice by blocking microsomal metabolism. Compounds in the series had low clearance and significant oral exposure in rats; therefore, a rat chronic infection model was used in parallel to assess the bactericidal activity of these compounds. Hence, our overall focus during the lead optimization phase was to identify analogues with improved metabolic stability across species, including mice, and to mitigate the PDE6 liability while maintaining or improving DprE1 inhibition and cellular activity.

Table 2. Structure–Activity Relationship of 1,4-Azaindole Analogues^a


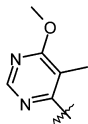
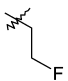
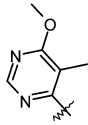
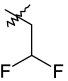
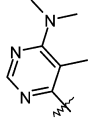
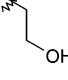
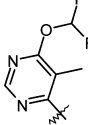
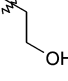
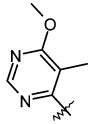
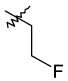
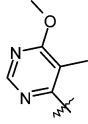
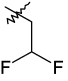
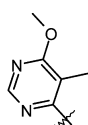
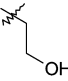
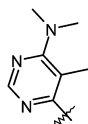
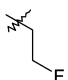
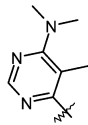
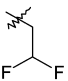
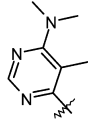
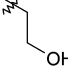
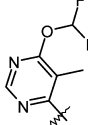
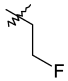
No	R1	R2	R3	Mtb MIC (μM)	DprE1 IC ₅₀ (μM)	Mouse microsomal Cl _{int} (μl/min/mg)	Measured logD
11	CH ₃			<0.39	0.003	107	2.6
17	CH ₃			<0.39	<0.005	77	2.9
18	CH ₃			<0.39	0.028	38	1.8
19	CH ₃			<0.39	0.021	26	2.0
20	OCH ₃			<0.39	0.013	129	2.5
21	OCH ₃			<0.39	0.009	106	2.8
22	OCH ₃			0.78	0.019	<24	1.6
23	OCH ₃			<0.39	0.007	50	2.2
24	OCH ₃			<0.39	0.003	>130	2.5
25	OCH ₃			<0.39	0.043	26	1.6
26	OCH ₃			<0.39	0.005	ND	2.2

Table 2. continued

No	R1	R2	R3	Mtb MIC (μ M)	DprE1 IC ₅₀ (μ M)	Mouse microsomal Cl _{int} (μ l/min/mg)	Measured logD
27	OCH ₃			<0.39	0.005	ND	2.4
28	OCH ₃			0.78	0.017	9	1.5
29	CH ₃			<0.39	0.011	22	2.2
30	CH ₃			<0.39	0.015	ND	2.4
31	F			6.25	ND*	ND	ND*
32	Br			1.56	0.022	ND	2.4
33	CF ₃			>200	0.2	ND	ND*
34	Cyclopropyl			3.12	0.013	ND	3.1
35				6.25	0.012	ND	>4.9
36				>100	ND	ND	>4.1
37				<0.39	0.019	102	3.3

ND, not determined; ND, precipitated under assay conditions.

In this article, we describe our strategy for identifying improved DprE1 inhibitors that have potent cellular activity, good oral exposure across species, and minimal in vitro safety risks. We also demonstrate that 1,4-azaindoles are efficacious in a rat chronic infection model. We believe that these optimized compounds from the 1,4-azaindole series are suitable for in vivo safety and combination studies with other antitubercular agents.

RESULTS AND DISCUSSION

To understand the SAR for PDE6 inhibition, structurally diverse compounds from the 1,4-azaindole series were profiled in an in vitro PDE6 assay (Table 1). The results revealed that the *N*-1,6-methoxy-5-methylpyrimidine-4-yl substituent was the primary cause of PDE6 activity (compounds 9–12 vs 13–16; Table 1). With a goal to mitigate PDE6 activity, we initially

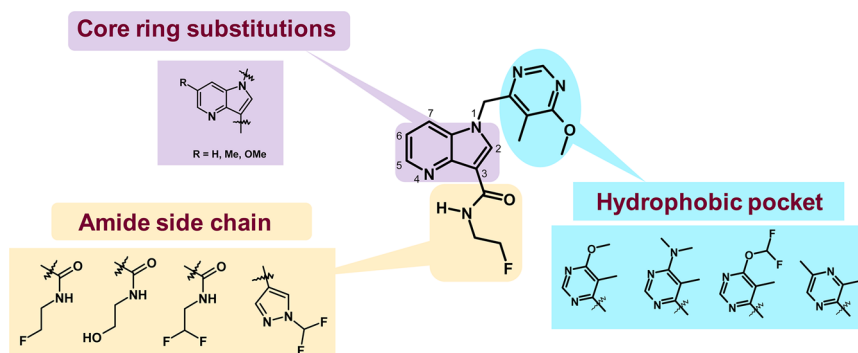


Figure 2. Optimized SAR and SPR for 1,4-azaindoles.

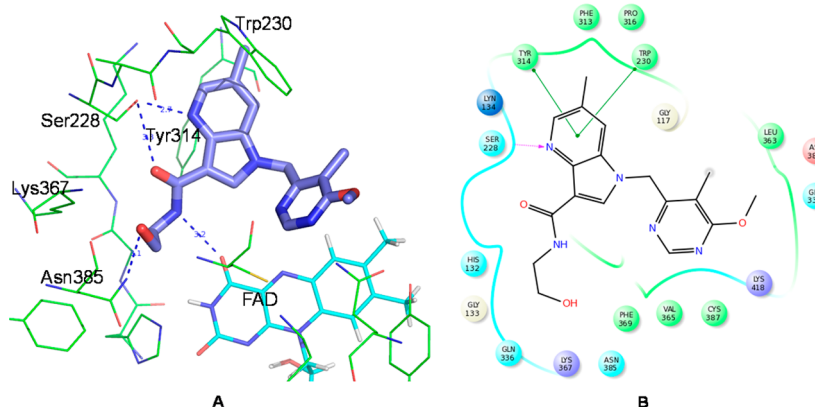


Figure 3. (A) Binding mode of compound 11 in the DprE1 active site. (B) Two-dimensional ligand interaction plot.

sought to replace the 6-methoxy-5-methylpyrimidine-4-yl substituent with groups that maintained the overall hydrophobic footprint and that act as a hydrogen-bond acceptor (Table 2). The syntheses of these analogues were straightforward, as shown in Scheme 1. As described earlier, synthesis of the azaindole core followed by alkylation with a variety of aryl halides and subsequent hydrolysis and amide coupling provided the desired analogues.³ The synthesis of some of the aryl halides required an additional manipulation (Supporting Information).

The DprE1 inhibition (IC_{50}) and Mtb cellular activities (minimum inhibitory concentration, MIC) were evaluated using biochemical and cellular assay, respectively. All compounds in the series have potent DprE1 enzyme inhibition and Mtb MIC's. Three points of diversification, namely, the amide side chain, a hydrophobic group, and core ring substitutions, were explored, as shown in Figure 2. The SAR and structure–property relationship (SPR) optimization is shown in Figure 2 and Tables 2 and 4. The aqueous solubility, microsomal stability, and PDE6 inhibition are influenced primarily by the amide side chain and the hydrophobic group (Figure 2). The hydrophilic amide side chain (hydroxyethyl) influences the physicochemical properties, which is evident from the high solubility values observed (Table 4). The hydroxyethyl amide side chain also showed a significant improvement in mouse liver microsome (MLM) stability relative to that with hydrophobic amide side chains. The high MLM instability is possibly due to the high lipophilicity (measured logD) rather than any specific metabolic softspot. Compounds with logD of 2 or less (18, 19, 22, 25, and 28) showed a remarkable improvement in MLM stability. The disubstituted heteroaryl-methyl group at the northern position is critical to modulate MIC, physicochemical, and in vitro safety

properties. It was observed that the replacement of the 6-methoxy-5-methylpyrimidine-4-yl substituent with a 6-(dimethylamino)-5-methylpyrimidine-4-yl or 6-(difluoromethoxy)-5-methylpyrimidine-4-yl substituent helped to mitigate PDE6 activity (compounds 9–12 vs 13–16; Table 1). Thus, the overall hydrophobic footprint and a hydrogen-bond acceptor are required for enzymatic and cellular activity. The C-6 substitution was found to be most favorable for cellular potency compared to that of C-5 and C-7 substitutions (compounds 17–30 vs 35–36; Table 1); however, the CF_3 group at the C-6 position (33) was not tolerated. The methyl or methoxy group at the C-6 position of the 1,4-azaindole helped to improve cellular potency (compounds 17–30 vs 31–34; Table 1), whereas bioisosteric replacement of the amide to a substituted pyrazole helped to retain both enzymatic and cellular potency (compound 37). Thus, the compounds from the 1,4-azaindole series have nanomolar IC_{50} 's, submicromolar MIC's, and the desired mouse microsomal stability, and they lack in vitro PDE6 safety liability.

In order to understand the possible mode of binding for azaindoles, we performed docking using Glide6.1.^{6,7} A series of seminal studies on the structural biology of DprE1 over the last 2 years has culminated in a number of ligand-bound crystal structures of *Mycobacterium smegmatis* (Msm) and Mtb.^{8–10} The crystal structure reported with one of the noncovalent inhibitors, TCA1,⁶ was used (PDB ID: 4KW5) for modeling. The docking without constraints suggested multiple binding modes; one of the major binding modes is shown in Figure 3. Tyr314, the residue that was mutated by azaindole, is involved in a C–H– π van der Waals contact with the azaindole ring. The N atom of the pyridyl ring in azaindole forms an H-bond with Ser 228. The amide carbonyl oxygen is within H-bonding

distance from the Ser 228 –OH group and thus can participate in bifurcated H-bonding along with the N atom of the pyridyl ring. The NH group of the amide is within H-bonding distance from the FAD ring carbonyl oxygen. The terminal OH/F atom makes a H-bonding contact with the amide NH of Asn385. Thus, Tyr314, Ser228, and Asn385 are the key residues involved in binding interactions with 1,4-azaindoles.

Spontaneous resistant mutants to compounds **11** and **12** arose at a frequency of $4\text{--}7 \times 10^{-7}$ at 4–16 times MIC. Mutant strains showed a >100-fold upward shift in MIC with respect to that of the wild-type H37Rv strain. A single-nucleotide change in *dprE1* (Rv3790), resulting in an amino acid substitution (Tyr → His) at position 314, was found by genome sequencing of the resistant Mtb mutants. This was the same mutation that was previously observed in all of the resistant strains raised against two early 1,4-azaindole compounds.³ Although no significant secondary targets were observed for earlier compounds, resistant strains raised against compounds **11** and **12** had an additional mutation in Rv1937 that resulted in an amino acid substitution (Phe → Cys) at position 462. Rv1937, an oxygenase, has been shown to be nonessential by TraSH transposon mutagenesis.¹¹ Also, the DprE1 Y314H strain imparts a similar degree of resistance compared to that of strains with mutations in two loci. Hence, the contribution of Rv1937 F426C toward imparting resistance to 1,4-azaindoles is unclear. For these mutant strains, as reported previously, compounds within the series were cross-resistant; however, the strains were still susceptible to **1** (Table 3).³ On the other hand, benzothiazinone-resistant strains

DprE1 C387G and C387S are sensitive to 1,4-azaindoles. Although **1** and 1,4-azaindoles share the same target, these studies indicate that they have different patterns of interaction with the target binding site.

In vitro drug metabolism and pharmacokinetic (DMPK) and physicochemical properties of the representative compounds are shown in Table 4. Measurement of aqueous solubility from DMSO-dried solids for compounds **12**, **18**, **19**, **22**, and **25** was greater than that for compounds **11** and **17**; the improved solubility can be attributed to the hydroxyethyl amide side chain. On the basis of in vitro intrinsic clearance (CL_{int}) using human microsomes and rat hepatocytes, the predicted in vivo clearance (CL) for compounds **11**, **12**, **17**, **18**, **19**, **22**, and **25** ranged between 8 and 30% of liver blood flow (% LBF), indicating low metabolic turnover. In contrast, the in vitro intrinsic clearance was higher from mouse microsomes for compounds **11** and **17** than it was for compounds **18**, **19**, **22**, and **25** (Table 2), suggesting an influence of the hydroxyethyl amide side chain on the possible species-specific clearance mechanism. The compounds were found to be highly permeable and did not inhibit cytochrome P450 (CYP) enzymes. No major safety liabilities were identified for the 1,4-azaindole series when tested against a panel of mammalian targets and hERG channel. However, compounds **11**, **12**, and **22** showed modest PDE6 inhibition.

In vivo PK measurements in rats showed good oral exposure, low-to-moderate CL (12–48 mL/min/kg), and good (>60%) oral bioavailability. Compounds **11** and **17** were assessed for in vivo efficacy in Wistar rats in a chronic TB infection model.¹² After 4 weeks of treatment with these compounds, the bacterial burden in the lungs was reduced by ~1 log CFU compare to that of the untreated control group (Figure 4A). The observed efficacy in the chronic TB infection model was supported by the exposures measured in infected animals (AUCs: 23 to 98 $\mu\text{M}\cdot\text{h}$) and free plasma concentrations (above MIC for 10–24 h) (Figure 4B). During the 4 weeks of repeated dosing in the efficacy study, no adverse events were observed. Body weight, organ weight, and gross pathology were found to be unaffected.

As described above, compounds such as **11** and **17** were rapidly metabolized in the presence of mouse liver microsomes, leading to low exposures in mice along with a poor PK profile. Our medicinal chemistry exploration identified compounds **12**, **18**, **22**, and **25** as having low in vitro clearance in the presence of mouse liver microsomes. Therefore, these compounds were profiled for in vivo PK assessment in mice to help establish in

Table 3. Cross-Resistance of 1,4-Azaindoles

compd	Mtb MIC (μM)					
	H37Rv	DprE1 OE	DprE1 C387S	DprE1 C387G	DprE1 Y314H	DprE1 Y314H Rv1937 F426C
11	0.39	12.5	0.39	0.39	>100	>100
12	0.78	>100	0.78	0.78	>100	>100
17	<0.39	>100	ND	ND	>100	>100
18	0.39	>100	0.39	0.39	>100	>100
19	0.78	100	0.78	0.78	>100	>100
22	1.56	>100	1.56	1.56	>100	>100
25	0.39	>100	0.39	0.39	>100	>100
1	0.0015	12.5	12.5	25	0.0015	0.003
RIF	0.004	0.004	0.004	0.004	0.002	0.004
INH	0.312	0.156	0.625	0.312	0.625	0.625
Moxi	0.125	0.125	0.125	0.125	0.125	0.125

Table 4. 1,4-Azaindoles: DMPK and Safety Properties^a

	11	12	17	18	19	22	25
logD	2.6	1.8	2.95	1.8	2	1.6	1.6
solubility (μM)	4	170	3	464	68	315	129
human CL_{pred} microsomes (% LBF)	15	19	16	30	20	16	29
rat CL_{pred} hepatocytes (% LBF)	12	14	9	16	16	8	16
human PPB (% free)	7	22	5	30	30	17	30
Caco-2 A-B/B-A (1×10^{-6} cm/s)	33/18	11/30	24/9	5/37	13/23	11/31	3/39
CYP inhibition (μM) ^b	>50	>50	>50	>50	>50	>50	>50
hERG (μM)	>33	>33	>33	>33	>33	>33	>33
PDE6 IC_{50} (μM)	1	4	>10	>100	>100	2	>100
secondary pharmacology hits IC_{50} (μM)	no significant hits ^c						
rat PK	CL (mL/min/kg)	14	27	ND	48	12	16
	F (%)	80	100		64	100	87

^aND, not determined. ^bCYP1A2, CYP2C9, CYP2C19, CYP2D6, and CYP3A4. ^cPanel of ~65 high- and medium-severity targets (binding and functional data); $IC_{50} > 100 \mu\text{M}$ or $> 30 \mu\text{M}$

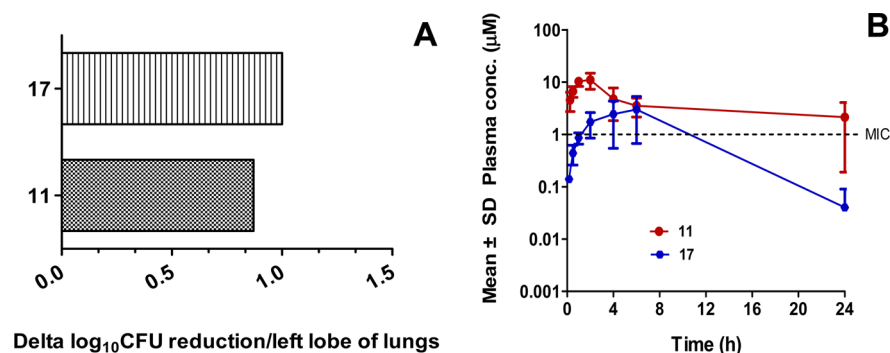


Figure 4. (A) Summary of efficacy of **11** and **17** in a chronic TB infection model in Wistar Rats following 6 days/week PO dosing at 100 mg/kg for 4 weeks. The net log CFU reduction/left lobe of the lungs was obtained by subtracting lung bacterial counts from that of the vehicle treated controls. Both compounds exhibited a statistically significant effect vs untreated controls ($p < 0.05$). (B) Time vs concentration profiles of **11** and **17** following multiple oral administrations at 100 mg/kg in chronically Mtb infected rats.

vitro to in vivo correlations (IVIVE). All four compounds exhibited good oral exposure in mice, thus confirming IVIVE (Figure 5 and Table 5).

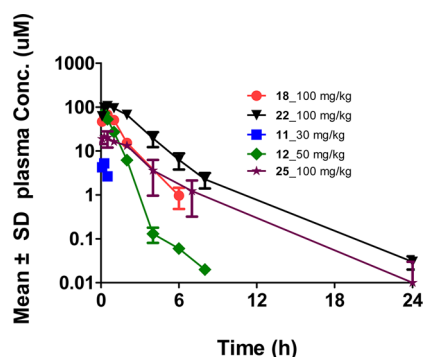


Figure 5. Time vs concentration profiles of **11**, **12**, **18**, **22**, and **25** following single oral dose administrations in healthy BALB/c mice.

Table 5. Pharmacokinetic Parameters of **11**, **12**, **18**, **22**, and **25** Following Single Oral Dose Administration in BALB/c Mice^a

PK parameter	compd				
	11	12	18	22	25
dose (mg/kg)	30	50	100	100	100
C_{max} (μM)	5.24	73 ± 2	70 ± 3	105 ± 8	23 ± 5
t_{max} (h)	0.25	0.25 ± 0	0.4 ± 0.9	0.5 ± 0	0.3 ± 0.2
AUC _{inf} (μM·h)	2	62 ± 4	106 ± 5	286 ± 41	57 ± 9
$t_{1/2}$ (h)	0.5	0.7 ± 0.3	0.9 ± 0.2	2 ± 0.3	2 ± 1

^aMean ± SD; $n = 3$.

In summary, we have successfully mitigated the challenge of metabolic instability and PDE6 inhibition associated with 1,4-azaindoles, while retaining potent DprE1 inhibition and cellular activity. We believe that these optimized compounds have the potential to deliver a candidate drug for TB.

EXPERIMENTAL SECTION

All chemicals, reagent grade solvents, and anhydrous solvents were purchased from either Sigma-Aldrich Chemical Co. or Fisher Scientific. All reactions were conducted under nitrogen unless otherwise noted. Solvents were removed in vacuo on a rotary evaporator. Thin-layer chromatography was performed to monitor reactions using precoated Merck Silica Gel 60 F254 plates and

visualized by UV light. Flash column chromatography was performed using silica cartridges purchased from Grace Purification systems. All compounds were analyzed for purity by HPLC and characterized by ¹H NMR using Bruker 300 MHz NMR and/or Bruker 400 MHz NMR spectrometers. Chemical shifts are reported in ppm (δ) relative to the residual solvent peak in the corresponding spectra: chloroform, δ 7.26; methanol, δ 3.31; DMSO, δ 3.33. Coupling constants (J) are reported in hertz (Hz), where s, singlet; br s, broad singlet; d, doublet; dd, double doublet; bd, broad doublet; ddd, double doublet of doublets; t, triplet; tt, triplet of triplets; q, quartet; and m, multiplet, and were analyzed using ACD NMR data processing software. Mass spectra values are reported as m/z . All final compounds for biological testing were purified by reverse-phase HPLC with >95% purity [Shimadzu HPLC instrument with a Hamilton reversed-phase column (HxSil, C18, 3 μm, 2.1 mm × 50 mm (H2)). Eluent A: 5% CH₃CN in H₂O; eluent B: 90% CH₃CN in H₂O. A flow rate of 0.2 mL/min was used with UV detection at 254 and 214 nm].

N-(2-Fluoroethyl)-1-((6-methoxy-5-methylpyrimidin-4-yl)methyl)-1H-pyrrolo[3,2-b]pyridine-3-carboxamide (9). MS (ES⁺) m/z : 344. ¹H NMR (300 MHz, DMSO- d_6): δ 2.24 (s, 3H), 3.67 (d, $J = 5.46$ Hz, 1H), 3.76 (d, $J = 5.46$ Hz, 1H), 3.93 (s, 3H), 4.50 (t, $J = 4.99$ Hz, 1H), 4.66 (t, $J = 4.99$ Hz, 1H), 5.69 (s, 2H), 7.26 (dd, $J = 8.29$, 4.71 Hz, 1H), 7.94 (d, $J = 8.52$ Hz, 1H), 8.28 (s, 1H), 8.41 (s, 1H), 8.49 (d, $J = 4.57$ Hz, 1H), 8.95 (s, $J = 5.89$, 5.89 Hz, 1H). HRMS (M + H) calcd for C₁₇H₁₈FN₅O₂, 344.1517; found, 344.15242.

N-(Cyclopropylmethyl)-1-((6-methoxy-5-methylpyrimidin-4-yl)methyl)-1H-pyrrolo[3,2-b]pyridine-3-carboxamide (10). MS (ES⁺) m/z : 352. ¹H NMR (300 MHz, DMSO- d_6): δ 0.02 (q, $J = 4.58$ Hz, 2H), 0.18–0.31 (m, 2H), 0.83 (t, $J = 6.88$ Hz, 1H), 2.00 (s, 3H), 2.98–3.11 (m, 3H), 3.69 (s, 3H), 5.43 (s, 2H), 7.00 (dd, $J = 8.29$, 4.71 Hz, 1H), 7.68 (dd, $J = 8.29$, 1.13 Hz, 1H), 7.98 (s, 1H), 8.17 (s, 1H), 8.24 (dd, $J = 4.71$, 1.13 Hz, 1H), 8.55 (t, $J = 5.75$ Hz, 1H). HRMS (M + H) calcd for C₁₉H₂₁FN₅O₂, 352.17677; found, 352.17712.

N-(2-Fluoroethyl)-1-((6-methoxy-5-methylpyrimidin-4-yl)methyl)-6-methyl-1H-pyrrolo[3,2-b]pyridine-3-carboxamide (11). MS (ES⁺) m/z : 358. ¹H NMR (300 MHz, DMSO- d_6): δ 2.17–2.30 (3, 3H), 2.40 (s, 3H), 3.59–3.73 (m, 1H), 3.73–3.83 (m, 1H), 3.94 (s, 3H), 4.50 (t, $J = 4.99$ Hz, 1H), 4.66 (t, $J = 4.99$ Hz, 1H), 5.64 (s, 2H), 7.76 (s, 1H), 8.15 (s, 1H), 8.35 (s, 1H), 8.42 (s, 1H), 8.87 (t, $J = 5.84$ Hz, 1H). HRMS (M + H) calcd for C₁₈H₂₀FN₅O₂, 358.16735; found, 358.16808.

N-(2-Hydroxyethyl)-1-((6-methoxy-5-methylpyrimidin-4-yl)methyl)-6-methyl-1H-pyrrolo[3,2-b]pyridine-3-carboxamide (12). MS (ES⁺) m/z : 356. ¹H NMR (300 MHz, DMSO- d_6): δ 2.23 (s, 3H), 2.39 (s, 3H), 3.39–3.65 (m, 4H), 3.93 (s, 3H), 4.84 (t, $J = 5.09$ Hz, 1H), 5.63 (s, 2H), 7.74 (s, 1H), 8.12 (s, 1H), 8.33 (s, 1H), 8.41 (s, 1H), 8.80 (t, $J = 5.65$ Hz, 1H). HRMS (M + H) calcd for C₁₈H₂₁FN₅O₃, 356.17168; found, 356.17200.

1-((6-(Dimethylamino)-5-methylpyrimidin-4-yl)methyl)-N-(2-fluoroethyl)-1H-pyrrolo[3,2-b]pyridine-3-carboxamide (13). MS (ES⁺) m/z : 357. ¹H NMR (400 MHz, DMSO- d_6): δ 2.27 (s, 3H),

3.32 (s, 6H), 3.68 (q, $J = 5.1$ Hz, 1H), 3.75 (q, $J = 5.2$ Hz, 1H), 4.52 (t, $J = 5.0$ Hz, 1H), 4.64 (t, $J = 5.0$ Hz, 1H), 5.59 (s, 1H), 7.24 (dd, $J = 4.7, 8.3$ Hz, 1H), 7.92 (d, $J = 8.4$ Hz, 1H), 8.22 (s, 1H), 8.24 (s, 1H), 8.47 (d, $J = 4.6$ Hz, 1H), 8.94 (t, $J = 5.6$ Hz, 1H). HRMS ($M + H$) calcd for $C_{18}H_{21}FN_6O$, 357.18333; found, 357.18395.

(S)-1-((5-Fluoro-2-methoxypyridin-3-yl)methyl)-N-(2-fluoropropyl)-6-methyl-1H-pyrrolo[3,2-*b*]pyridine-3-carboxamide (14). MS (ES^+) m/z : 375. 1H NMR (300 MHz, DMSO- d_6): δ 1.24–1.37 (m, 3H), 2.44 (s, 3H), 3.47 (s, 1H), 3.64 (br s, 1H), 3.75 (s, 1H), 3.90 (s, 3H), 4.76 (br s, 1H), 4.90 (br s, 1H), 5.42 (s, 2H), 7.38 (s, 1H), 7.93 (s, 1H), 8.12 (d, $J = 3.01$ Hz, 1H), 8.23 (s, 1H), 8.38 (s, 1H), 8.90 (s, 1H). HRMS ($M + H$) calcd for $C_{19}H_{20}F_2N_4O_2$, 375.16267; found, 375.16286.

N-(2-Hydroxyethyl)-1-((2-methoxy-5-(trifluoromethyl)pyridin-3-yl)methyl)-6-methyl-1H-pyrrolo[3,2-*b*]pyridine-3-carboxamide (15). MS (ES^+) m/z : 409. 1H NMR (300 MHz, DMSO- d_6): δ 2.43 (s, 3H), 3.40–3.48 (m, 2H), 3.49–3.59 (m, 2H), 3.98 (s, 3H), 4.79–4.89 (m, 1H), 5.47 (s, 2H), 7.75–7.81 (m, 1H), 7.94 (s, 1H), 8.22 (s, 1H), 8.36 (d, $J = 1.32$ Hz, 1H), 8.56 (d, $J = 1.13$ Hz, 1H), 8.75–8.85 (m, 1H). HRMS ($M + H$) calcd for $C_{19}H_{19}F_3N_4O_3$, 409.14817; found, 409.1489.

N-(2-Fluoroethyl)-6-methyl-1-((3-methyl-4-(2,2,2-trifluoroethoxy)pyridin-2-yl)methyl)-1H-pyrrolo[3,2-*b*]pyridine-3-carboxamide (16). MS (ES^+) m/z : 425. 1H NMR (300 MHz, DMSO- d_6): δ 2.24 (s, 3H), 2.39 (s, 3H), 3.66 (q, $J = 5.21$ Hz, 1H), 3.75 (q, $J = 5.15$ Hz, 1H), 4.49 (t, $J = 4.99$ Hz, 1H), 4.65 (t, $J = 4.99$ Hz, 1H), 4.90 (q, $J = 8.85$ Hz, 2H), 5.63 (s, 2H), 7.07 (d, $J = 5.65$ Hz, 1H), 7.76 (s, 1H), 8.11 (s, 1H), 8.17 (d, $J = 5.65$ Hz, 1H), 8.34 (s, 1H), 8.88 (t, $J = 5.84$ Hz, 1H). HRMS ($M + H$) calcd for $C_{20}H_{20}F_4N_4O_2$, 425.15948; found, 425.16032.

N-(2,2-Difluoroethyl)-1-((6-methoxy-5-methylpyrimidin-4-yl)methyl)-6-methyl-1H-pyrrolo[3,2-*b*]pyridine-3-carboxamide (17). MS (ES^+) m/z : 376. 1H NMR (300 MHz, DMSO- d_6): δ 2.18–2.31 (m, 3H), 2.40 (s, 3H), 3.84–3.97 (m, 5H), 5.62–5.70 (m, 2H), 6.01–6.22 (tt, 1H), 7.78 (s, 1H), 8.20 (s, 1H), 8.38–8.41 (d, $J = 14.51$ Hz, 2H), 8.87–8.96 (m, 1H). HRMS ($M + H$) calcd for $C_{18}H_{19}F_2N_5O_2$, 376.15792; found, 376.1579.

1-((6-(Dimethylamino)-5-methylpyrimidin-4-yl)methyl)-N-(2-hydroxyethyl)-6-methyl-1H-pyrrolo[3,2-*b*]pyridine-3-carboxamide (18). MS (ES^+) m/z : 369. 1H NMR (300 MHz, DMSO- d_6): δ 2.27 (s, 3H), 2.40 (s, 3H), 2.95 (s, 6H), 3.41–3.58 (m, 4H), 4.84 (t, $J = 4.99$ Hz, 1H), 5.53 (s, 2H), 7.73 (s, 1H), 8.10 (s, 1H), 8.22 (s, 1H), 8.33 (s, 1H), 8.80 (t, $J = 5.46$ Hz, 1H). HRMS ($M + H$) calcd for $C_{19}H_{24}N_6O_2$, 369.20331; found, 369.20369.

1-((6-(Difluoromethoxy)-5-methylpyrimidin-4-yl)methyl)-N-(2-hydroxyethyl)-6-methyl-1H-pyrrolo[3,2-*b*]pyridine-3-carboxamide (19). MS (ES^+) m/z : 392. 1H NMR (400 MHz, DMSO- d_6): δ 2.32 (s, 3H), 2.40 (s, 3H), 3.46 (d, $J = 5.6$ Hz, 2H), 3.56 (d, $J = 5.1$ Hz, 2H), 5.75 (s, 2H), 4.83 (brs, 1H), 8.02–7.53 (m, 2H), 8.21–8.04 (m, 1H), 8.35 (s, 1H), 8.52 (s, 1H), 8.81 (br s, 1H). HRMS ($M + H$) calcd for $C_{18}H_{19}F_2N_5O_3$, 392.15284; found, 392.15328.

N-(2-Fluoroethyl)-6-methoxy-1-((6-methoxy-5-methylpyrimidin-4-yl)methyl)-1H-pyrrolo[3,2-*b*]pyridine-3-carboxamide (20). MS (ES^+) m/z : 374. 1H NMR (300 MHz, DMSO- d_6): δ 2.14–2.32 (m, 3H), 3.64–3.86 (m, 5H), 3.94 (s, 3H), 4.49 (t, $J = 4.99$ Hz, 1H), 4.65 (t, $J = 4.90$ Hz, 1H), 5.64 (s, 2H), 7.63 (d, $J = 2.45$ Hz, 1H), 8.07 (s, 1H), 8.26 (d, $J = 2.45$ Hz, 1H), 8.43 (s, 1H), 8.76 (t, $J = 5.93$ Hz, 1H). HRMS ($M + H$) calcd for $C_{18}H_{20}FN_5O_3$, 374.16226; found, 374.16291.

N-(2,2-Difluoroethyl)-6-methoxy-1-((6-methoxy-5-methylpyrimidin-4-yl)methyl)-1H-pyrrolo[3,2-*b*]pyridine-3-carboxamide (21). MS (ES^+) m/z : 392. 1H NMR (300 MHz, DMSO- d_6): δ 2.18–2.31 (m, 3H), 3.77–3.97 (m, 8H), 5.62–5.69 (m, 2H), 6.00–6.38 (tt, 1H), 7.64 (d, $J = 2.45$ Hz, 1H), 8.11 (s, 1H), 8.27 (d, $J = 2.45$ Hz, 1H), 8.43 (s, 1H), 8.74–8.84 (m, 1H). HRMS ($M + H$) calcd for $C_{18}H_{19}F_2N_5O_3$, 392.15284; found, 392.15328.

N-(2-Hydroxyethyl)-6-methoxy-1-((6-methoxy-5-methylpyrimidin-4-yl)methyl)-1H-pyrrolo[3,2-*b*]pyridine-3-carboxamide (22). MS (ES^+) m/z : 372. 1H NMR (300 MHz, DMSO- d_6): δ 2.23 (s, 3H), 3.31–3.43 (m, 4H), 3.81 (s, 3H), 3.94 (s, 3H), 4.83 (t, $J = 4.99$ Hz, 1H), 5.63 (s, 2H), 7.61 (d, $J = 2.45$ Hz, 1H), 8.03 (s, 1H), 8.25

(d, $J = 2.45$ Hz, 1H), 8.43 (s, 1H), 8.64–8.74 (m, 1H). HRMS ($M + H$) calcd for $C_{18}H_{21}F_2N_5O_4$, 372.1666; found, 372.16642.

1-((6-(Dimethylamino)-5-methylpyrimidin-4-yl)methyl)-N-(2-fluoroethyl)-6-methoxy-1H-pyrrolo[3,2-*b*]pyridine-3-carboxamide (23). MS (ES^+) m/z : 387. 1H NMR (400 MHz, DMSO- d_6): δ 2.28 (s, 3H), 2.96 (s, 6H), 3.67 (q, $J = 5.2$ Hz, 1H), 3.74 (q, $J = 5.4$ Hz, 1H), 3.83 (s, 3H), 4.51 (t, $J = 5.0$ Hz, 1H), 4.63 (t, $J = 5.0$ Hz, 1H), 5.55 (s, 2H), 7.62 (d, $J = 2.4$ Hz, 1H), 8.05 (s, 1H), 8.27–8.25 (m, 2H), 8.77 (t, $J = 6.0$ Hz, 1H). HRMS ($M + H$) calcd for $C_{19}H_{23}FN_6O_2$, 387.19389; found, 387.19384.

N-(2,2-Difluoroethyl)-1-((6-(dimethylamino)-5-methylpyrimidin-4-yl)methyl)-6-methoxy-1H-pyrrolo[3,2-*b*]pyridine-3-carboxamide (24). MS (ES^+) m/z : 405. 1H NMR (400 MHz, DMSO- d_6): δ 2.27 (s, 3H), 2.95 (s, 6H), 4.00–3.84 (m, 5H), 5.55 (s, 2H), 6.32–6.04 (m, 1H), 7.62 (d, $J = 2.3$ Hz, 1H), 8.08 (s, 1H), 8.27–8.24 (m, 2H), 8.79 (t, $J = 6.0$ Hz, 1H). HRMS ($M + H$) calcd for $C_{19}H_{22}F_2N_6O_2$, 405.18447; found, 405.18516.

1-((6-(Dimethylamino)-5-methylpyrimidin-4-yl)methyl)-N-(2-hydroxyethyl)-6-methoxy-1H-pyrrolo[3,2-*b*]pyridine-3-carboxamide (25). MS (ES^+) m/z : 385. 1H NMR (400 MHz, DMSO- d_6): δ 2.28 (s, 3H), 2.96 (s, 6H), 3.46–3.43 (m, 2H), 3.55–3.54 (m, 2H), 3.82 (s, 3H), 4.82 (br s, 1H), 5.54 (s, 2H), 7.60 (d, $J = 2.4$ Hz, 1H), 8.01 (s, 1H), 8.37–8.17 (m, 2H), 8.69 (t, $J = 5.7$ Hz, 1H). HRMS ($M + H$) calcd for $C_{19}H_{24}N_6O_3$, 385.19823; found, 385.19822.

1-((6-(Difluoromethoxy)-5-methylpyrimidin-4-yl)methyl)-N-(2-fluoroethyl)-6-methoxy-1H-pyrrolo[3,2-*b*]pyridine-3-carboxamide (26). MS (ES^+) m/z : 410. 1H NMR (400 MHz, DMSO- d_6): δ 2.31 (s, 3H), 3.68–3.67 (m, 1H), 3.77–3.71 (m, 1H), 3.82 (s, 3H), 4.52 (t, $J = 4.9$ Hz, 1H), 4.64 (t, $J = 4.9$ Hz, 1H), 5.75 (s, 2H), 7.99–7.63 (m, 2H), 8.09 (s, 1H), 8.27 (d, $J = 2.2$ Hz, 1H), 8.54 (s, 1H), 8.78 (t, $J = 5.7$ Hz, 1H). HRMS ($M + H$) calcd for $C_{18}H_{18}F_3N_5O_3$, 410.14342; found, 410.14421.

N-(2,2-Difluoroethyl)-1-((6-(difluoromethoxy)-5-methylpyrimidin-4-yl)methyl)-6-methoxy-1H-pyrrolo[3,2-*b*]pyridine-3-carboxamide (27). MS (ES^+) m/z : 428. 1H NMR (400 MHz, DMSO- d_6): δ 2.32 (s, 3H), 3.90–3.82 (m, 5H), 5.76 (s, 2H), 6.34–6.05 (m, 1H), 7.99–7.63 (m, 2H), 8.13 (s, 1H), 8.29 (d, $J = 2.4$ Hz, 1H), 8.81 (t, $J = 6.2$ Hz, 1H), 8.54 (s, 1H), 8.81 (t, $J = 6.2$ Hz, 1H). HRMS ($M + H$) calcd for $C_{18}H_{17}F_4N_5O_3$, 428.134; found, 428.13468.

1-((6-(Difluoromethoxy)-5-methylpyrimidin-4-yl)methyl)-N-(2-hydroxyethyl)-6-methoxy-1H-pyrrolo[3,2-*b*]pyridine-3-carboxamide (28). MS (ES^+) m/z : 408. 1H NMR (400 MHz, DMSO- d_6): δ 2.30 (s, 3H), 3.46–3.42 (m, 2H), 3.56–3.52 (m, 2H), 3.82 (s, 3H), 4.81 (t, $J = 5.0$ Hz, 1H), 5.73 (s, 2H), 7.97–7.61 (m, 2H), 8.04 (s, 1H), 8.25 (d, $J = 2.3$ Hz, 1H), 8.53 (s, 1H), 8.69 (t, $J = 5.6$ Hz, 1H). HRMS ($M + H$) calcd for $C_{18}H_{19}F_2N_5O_4$, 408.14775; found, 408.14848.

1-((3,5-Dimethylpyrazin-2-yl)methyl)-N-(2-fluoroethyl)-6-methyl-1H-pyrrolo[3,2-*b*]pyridine-3-carboxamide (29). MS (ES^+) m/z : 342. 1H NMR (300 MHz, DMSO- d_6): δ 2.40 (d, $J = 0.94$ Hz, 6H), 2.58 (s, 4H), 3.63–3.70 (m, 1H), 3.75 (q, $J = 5.53$ Hz, 1H), 4.49 (t, $J = 4.99$ Hz, 1H), 4.65 (t, $J = 5.18$ Hz, 1H), 5.67 (s, 2H), 7.75–7.79 (m, 1H), 8.12–8.17 (m, 2H), 8.33–8.37 (m, 1H), 8.87 (t, $J = 5.93$ Hz, 1H). HRMS ($M + H$) calcd for $C_{18}H_{20}FN_5O$, 342.17243; found, 342.17312.

N-(2,2-Difluoroethyl)-1-((3,5-dimethylpyrazin-2-yl)methyl)-6-methyl-1H-pyrrolo[3,2-*b*]pyridine-3-carboxamide (30). MS (ES^+) m/z : 360. 1H NMR (300 MHz, DMSO- d_6): δ 2.39 (s, 6H), 2.58 (s, 3H), 3.76–3.95 (m, 2H), 5.68 (s, 2H), 5.98–6.05 (m, 1H), 6.15–6.22 (m, 1H), 6.35–6.40 (m, 1H), 7.78 (s, 1H), 8.14 (s, 1H), 8.19 (s, 1H), 8.36 (s, 1H), 8.85–8.97 (m, 1H). HRMS ($M + H$) calcd for $C_{18}H_{19}F_2N_5O$, 360.16301; found, 360.1629.

6-Fluoro-N-(2-fluoroethyl)-1-((6-methoxy-5-methylpyrimidin-4-yl)methyl)-1H-pyrrolo[3,2-*b*]pyridine-3-carboxamide (31). MS (ES^+) m/z : 362. 1H NMR (300 MHz, DMSO- d_6): δ 2.25 (s, 3H), 3.62–3.80 (m, 2H), 3.98 (s, 3H), 4.48–4.70 (m, 2H), 5.68 (s, 2H), 8.0–8.10 (m, 1H), 8.30 (s, 1H), 8.41 (s, 1H), 8.55 (s, 1H), 8.66–8.72 (t, 1H).

6-Bromo-N-(2-fluoroethyl)-1-((6-methoxy-5-methylpyrimidin-4-yl)methyl)-1H-pyrrolo[3,2-*b*]pyridine-3-carboxamide (32). MS (ES^+) m/z : 423. 1H NMR (400 MHz, DMSO- d_6): δ 2.24 (s, 3H), 3.68 (br s, 1H), 3.75 (br s, 1H), 4.51 (br s, 1H), 4.64 (br s, 1H),

5.70 (s, 2H), 8.28 (s, 1H), 8.39 (d, 1H, $J = 10.9$ Hz), 8.58 (s, 1H), 8.64 (br s, 2H).

N-(2-Fluoroethyl)-1-((6-methoxy-5-methylpyrimidin-4-yl)methyl)-6-(trifluoromethyl)-1H-pyrrolo[3,2-b]pyridine-3-carboxamide (33). MS (ES^+) m/z : 412. 1H NMR (300 MHz, DMSO- d_6): δ 2.25 (s, 3H), 3.66–3.82 (m, 2H), 3.94 (s, 3H), 4.51 (s, 1H), 4.67 (s, 1H), 5.82 (s, 2H), 8.38 (s, 1H), 8.47–8.58 (m, 2H), 8.76 (br s, 1H), 8.85 (s, 1H).

6-Cyclopropyl-N-(2-fluoroethyl)-1-((6-methoxy-5-methylpyrimidin-4-yl)methyl)-1H-pyrrolo[3,2-b]pyridine-3-carboxamide (34). MS (ES^+) m/z : 384. 1H NMR (300 MHz, DMSO- d_6): δ 0.71–0.74 (m, 2H), 0.98–1.01 (m, 2H), 1.90–2.20 (m, 1H), 2.23 (s, 3H), 3.65–3.76 (m, 2H), 3.94 (s, 3H), 4.47–4.65 (m, 2H), 5.64 (s, 2H), 7.62 (s, 1H), 8.13 (s, 1H), 8.34–8.35 (m, 1H), 8.42 (s, 1H), 8.87 (s, 1H).

N-(Cyclopropylmethyl)-1-(5-fluoro-2-methoxybenzyl)-7-methyl-1H-pyrrolo[3,2-b]pyridine-3-carboxamide (35). MS (ES^+) m/z : 368. 1H NMR (300 MHz, DMSO- d_6): δ 0.22–0.24 (m, 2H), 0.48–0.50 (m, 2H), 1.05–1.09 (m, 1H), 2.44 (s, 3H), 3.28 (t, 2H, $J = 6.2$ Hz), 3.86 (s, 3H), 5.63 (s, 2H), 5.97–6.00 (m, 1H), 7.03–7.04 (m, 1H), 7.12–7.14 (m, 2H), 8.22 (s, 1H), 8.37 (d, 1H, $J = 4.8$ Hz), 9.01 (t, 1H, $J = 5.6$ Hz).

N-(Cyclopropylmethyl)-1-(2,4-dimethylbenzyl)-5-methoxy-1H-pyrrolo[3,2-b]pyridine-3-carboxamide (36). MS (ES^+) m/z : 364. 1H NMR (300 MHz, DMSO- d_6): δ 0.23–0.30 (m, 2H), 0.49–0.52 (m, 2H), 1.04–1.10 (m, 1H), 2.19 (s, 3H), 2.23 (s, 3H), 3.23–3.26 (m, 2H), 3.97 (s, 3H), 5.44 (s, 2H), 6.67–6.72 (m, 2H), 6.92–6.95 (m, 1H), 7.04 (s, 1H), 7.87–7.89 (m, 2H), 8.60–8.61 (m, 1H).

3-(1-(Difluoromethyl)-1H-pyrazol-4-yl)-1-((6-methoxy-5-methylpyrimidin-4-yl)methyl)-6-methyl-1H-pyrrolo[3,2-b]pyridine (37). MS (ES^+) m/z : 385. 1H NMR (300 MHz, DMSO- d_6): δ 2.24 (s, 3H), 2.41 (s, 3H), 3.94 (s, 3H), 5.55 (s, 2H), 7.69 (s, 1H), 7.94 (s, 1H), 8.29–8.35 (m, 2H), 8.46 (s, 1H), 8.75 (s, 1H). HRMS ($M + H$) calcd for $C_{19}H_{18}F_2N_6O$, 385.15826; found, 385.15793.

Biological Assays. Biological assay protocols for MIC determination, cytotoxicity, mutant generation, resistance frequency, whole-genome sequencing, DprE1 construct and protein purification, DprE1 enzyme assay and IC_{50} measurement, pharmacokinetics (PK) of azaindole compounds, in vivo efficacy studies, solubility assay, plasma protein binding assay, metabolic stability assay (mouse/human microsomal CL and rat/dog/human hepatocyte CL), logD, and hERG assay were described previously.^{3,12}

■ ASSOCIATED CONTENT

Supporting Information

Details of the synthesis of key intermediates and final compounds (35–37, 39–42, 44b, 45–47, and 49–55). This material is available free of charge via the Internet at <http://pubs.acs.org>.

■ AUTHOR INFORMATION

Corresponding Authors

*(P.S.S.) E-mail: psshirude@gmail.com. Tel.: +91 080 23621212. Fax: +91 080 23621214

*(M.C.) E-mail: monalisa.chatterji@astrazeneca.com.

Present Address

[∞]Sai Life Sciences Ltd, Pune 411057, India.

Notes

The authors declare no competing financial interest.

■ ACKNOWLEDGMENTS

This research was supported by the Global Alliance for TB Drug Development (GATB). We thank M. Jyothi for support with the DprE1 assay. We also thank Sunita DeSousa for coordinating this work with the TB alliance. Our sincere thanks to Global DMPK, Safety, Biosciences (AZ Boston, U.S.) and

Discovery Sciences (AZ, Alderly Park, U.K.) for technical support in various assays. We also thank Rajkumar and Subhash for animal welfare support. Our sincere thanks to G. Riccardi (University of Pavia) for providing the DprE1 expression plasmid.

■ ABBREVIATIONS USED

TB, tuberculosis; Mtb, *Mycobacterium tuberculosis*; DprE1, decaprenylphosphoryl- β -D-ribose-2'-epimerase 1; MDR-TB, multidrug-resistant tuberculosis; BTZs, nitro-benzothiazinones; DPR, decaprenylphosphoryl- β -D-ribose; DPA, decaprenylphosphoryl- β -D-arabinofuranose; DPX, decaprenylphosphoryl-2-keto- β -D-erythro-pentofuranose; MBC, minimum bactericidal concentration; MIC, minimum inhibitory concentration; SAR, structure–activity relationship; Msm, *Mycobacterium smegmatis*; DMPK, drug metabolism and pharmacokinetic; Cl_{int} , intrinsic clearance; PPB, plasma protein binding; CL, clearance; LBF, liver blood flow; CYP, cytochrome P450 enzymes; NMP, N-methyl pyrrolidine; HCl, hydrochloric acid; DMF, N,N-dimethylformamide; NaH, sodium hydride; EI, electrospray ionization; HRMS, high-resolution mass spectrometry

■ REFERENCES

- (1) *Global Tuberculosis Report 2013*; World Health Organization: Geneva, Switzerland, 2013.
- (2) Raviglione, M.; Marais, B.; Floyd, K.; Lönnroth, K.; Getahun, H.; Migliori, G. B.; Harries, A. D.; Nunn, P.; Lienhardt, C.; Graham, S.; Chakaya, J.; Weyer, K.; Cole, S.; Kaufmann, S. H.; Zumla, A. Scaling up interventions to achieve global tuberculosis control: progress and new developments. *Lancet* **2012**, 379, 1902–1913.
- (3) Shirude, P. S.; Shandil, R.; Sadler, C.; Naik, M.; Hosagrahara, V.; Hameed, S.; Shinde, V.; Bathula, C.; Humnabadkar, V.; Kumar, N.; Reddy, J.; Panduga, V.; Sharma, S.; Ambady, A.; Hegde, N.; Whiteaker, J.; McLaughlin, B.; Gardner, H.; Madhavapeddi, P.; Ramachandran, V.; Kaur, P.; Narayan, A.; Guptha, S.; Awasthy, D.; Narayan, C.; Mahadevaswamy, J.; Vishwas, K. G.; Ahuja, V.; Srivastava, A.; Prabhakar, K. R.; Bharath, S.; Kale, R.; Ramaiah, M.; Roy Choudhury, N.; Sambandamurthy, V.; Solapure, S.; Iyer, P.; Narayanan, S.; Chatterji, M. Azaindoles: noncovalent DprE1 inhibitors from scaffold morphing efforts, kill *Mycobacterium tuberculosis* and are efficacious in vivo. *J. Med. Chem.* **2013**, 56, 9701–9708.
- (4) Mikušová, K.; Huang, H.; Yagi, T.; Holsters, M.; Vereecke, D.; D'Haese, W.; Scherman, M. S.; Brennan, P. J.; McNeil, M. R.; Crick, D. C. Decaprenylphosphoryl arabinofuranose, the donor of the D-arabinofuranosyl residues of mycobacterial arabinan, is formed via a two step epimerization of decaprenylphosphoryl ribose. *J. Bacteriol.* **2005**, 187, 8020–8025.
- (5) Makarov, V.; Manina, G.; Mikušová, K.; Möllmann, U.; Ryabova, O.; Saint-Joanis, B.; Dhar, N.; Pasca, M. R.; Buroni, S.; Lucarelli, A. P.; Milano, A.; De Rossi, E.; Belanova, M.; Bobovska, A.; Dianiskova, P.; Kordulakova, J.; Sala, C.; Fullam, E.; Schneider, P.; McKinney, J. D.; Brodin, P.; Christophe, T.; Waddell, S.; Butcher, P.; Albrethsen, J.; Rosenkrands, I.; Brosch, R.; Nandi, V.; Bharath, S.; Gaonkar, S.; Shandil, R. K.; Balasubramanian, V.; Balganes, T.; Tyagi, S.; Grosset, J.; Riccardi, G.; Cole, S. T. Benzothiazinones kill *Mycobacterium tuberculosis* by blocking arabinan synthesis. *Science* **2009**, 324, 801–804.
- (6) *Glide6.1*, small-molecule drug discovery suite 2013-3; Schrödinger, LLC: New York, 2013.
- (7) Friesner, R. A.; Murphy, R. B.; Repasky, M. P.; Frye, L. L.; Greenwood, J. R.; Halgren, T. A.; Sanschagrin, P. C.; Mainz, D. T. Extra precision glide: docking and scoring incorporating a model of hydrophobic enclosure for protein–ligand complexes. *J. Med. Chem.* **2006**, 49, 6177–6196.
- (8) Makarov, V.; Lechartier, B.; Zhang, M.; Neres, J.; Van der Sar, A. M.; Raadsen, S. A.; Hartkoorn, R. C.; Ryabova, O. B.; Vocat, A.;

Decosterd, L. A.; Widmer, N.; Buclin, T.; Bitter, W.; Andries, K.; Pojer, F.; Dyson, P. J.; Cole, S. T. Towards a new combination therapy for tuberculosis with next generation benzothiazinones. *EMBO Mol. Med.* **2014**, *6*, 372–383.

(9) Neres, J.; Pojer, F.; Molteni, E.; Chiarelli, L. R.; Dhar, N.; Boy-Röttger, S.; Buroni, S.; Fullam, E.; Degiacomi, G.; Lucarelli, A. P.; Read, R. J.; Zaroni, G.; Edmondson, D. E.; De Rossi, E.; Pasca, M. R.; McKinney, J. D.; Dyson, P. J.; Riccardi, G.; Mattevi, A.; Cole, S. T.; Binda, C. Structural basis for benzothiazinone-mediated killing of *Mycobacterium tuberculosis*. *Sci. Transl. Med.* **2012**, *4*, 150ra121.

(10) Batt, S. M.; Jabeen, T.; Bhowruth, V.; Quill, L.; Lund, P. A.; Eggeling, L.; Alderwick, L. J.; Futterer, K.; Besra, G. S. Structural basis of inhibition of *Mycobacterium tuberculosis* DprE1 by benzothiazinone inhibitors. *Proc. Natl. Acad. Sci. U.S.A.* **2012**, *109*, 11354–11359.

(11) Sassetti, C. M.; Boyd, D. H.; Rubin, E. J. Genes required for mycobacterial growth defined by high density mutagenesis. *Mol. Microbiol.* **2003**, *48*, 77–84.

(12) Gaonkar, S.; Bharath, S.; Kumar, N.; Balasubramanian, V.; Shandil, R. K. Aerosol infection model of tuberculosis in Wistar rats. *Int. J. Microbiol.* **2010**, 426035.